

Switching-Controllable of Operational Transresistance Amplifier (OTRA) based Bistable Multivibrators

G. Shravan Kumar¹, J. Chandrashekar²

^{1,2}Assistant Professor

Department of Electronic and Communication Engineering
MLR Institute of Technology
Laxma Reddy Avenue, Dundigal, Hyderabad- 500043, India

Abstract: Two bistable multivibrators based on the operational transresistance amplifier (OTRA) are presented. The first topology consists of only one OTRA and a positive feedback network. The second multivibrator utilizes a single-pole double-throw (SPDT) switch along with a bias voltage source to shift the hysteresis loop into either the right-half-part or the left-half-part of the v_T - v_o plane. These two proposed circuits have a common attractive feature. That is, both clockwise and counter-clockwise hysteresis operations can be fulfilled with an additional SPDT switch connected to different configurations. In order to extend the applications, a general multiple-output configuration is also suggested. The presented bistable multivibrators are simple and versatile. The operation principles are described in detail. Theoretical analyses are verified by the experimental results on the prototype circuits.

Keywords: OTRA, Multivibrator, SPDT

1. Introduction

A bistable multivibrator, sometimes called Schmitt trigger, is widely used in many electronic fields, such as digital, instrumentation and measurement systems [1, 2]. Conventionally, an operational amplifier (OA) with a positive feedback connection is adopted to realise a bistable multivibrator. Apart from the voltage-mode approaches, another circuit design concept, current-mode technique, was introduced [3]. In 1968, the first current-based active device named current conveyor (CC) was proposed [4]. Since then, many new active devices have been reported in the literature [5–9]. Until now, the applications of current-mode technique in the analogue circuits have received much attention because these implementations help engineers to reduce design efforts and achieve multi-function features [10–11]. In the past few years, an active device called operational transresistance amplifier (OTRA) is reported and applied. Several OTRA-based implementations have emerged, such as active filters, oscillators and waveform generators [12–16].

In the previous researches, some novel bistable multivibrators are suggested [17–19]. Among them, one economic approach is based on a single operational transconductance amplifier (OTA) and a grounded resistor [18]. However, there exist two main drawbacks. The first one is that its output levels vary with the threshold voltages. The second limitation is that this circuit cannot fulfill a counter-clockwise (CCW) hysteresis characteristic. In order to overcome such problem, a similar topology, OTA-R Schmitt trigger, is presented in [19]. The authors use two OTAs and two grounded resistors to modify the previous design. Nevertheless, it is still impossible that both clockwise (CW) and CCW hysteresis functions are obtained.

On the basis of the above considerations, the OTRA is utilized as a main active device to present two general bistable multivibrators in this paper. Then several extended

circuits are designed. The proposed configurations feature two main advantages. The first is that it is very easy to obtain both hysteresis characteristics at the same topology with an additional SPDT switch. In addition, a second single-pole double-throw (SPDT) switch can be utilized to shift the hysteresis loop into either the right-half-part or the left-half-part of the v_i - v_o plane. This paper is organized as follows. In Section 2, the active device OTRA is introduced briefly. In Section 3, the first general configuration based on a single OTRA is described. Afterwards, two extended circuits are also discussed.

2. Realization of an OTRA

The OTRA is a three-port network, which is a high-gain current-input, voltage-output device [20–23]. The terminal relations of an OTRA can be expressed in (1). The circuit symbol of an OTRA is also shown in Fig. 1. The transresistance gain R_m is usually very large and can be treated as infinite in an ideal case.

$$\begin{aligned} V_+ &= 0 \\ V_- &= 0 \\ V_o &= I_+ R_m - I_- R_m \end{aligned} \quad (1)$$

In order to investigate the proposed circuits, the commercial IC AD844AN [24], which is a current-feedback OA (CFOA) [25], is adopted to implement an OTRA as shown in Fig. 2a [16]. To investigate the influences of the parasitic effects, the CFOA shown in Fig. 2a is treated as a second-generation current conveyor (CCII) cascading a voltage buffer with parasitic resistors at terminals. The parasitic resistances (R_{x_n}) of the inverting input terminals are in the order of several tens of ohms, whereas for the slewing nodes, the parasitic resistances (R_{z_n}) are of a few mega ohms. The equivalent circuit model with parasitic for the OTRA is depicted in Fig. 2b. It is observed that as long as R_{z1} and R_{z2} are kept as high as possible and R_{x1} and R_{x2} approach zero, a nearly ideal OTRA can be fulfilled with the adoption of either an

AD844AN IC or a CMOS CFOA. In the non-ideal model of the applied OTRA, the high input impedance R_{z2} of the slewing node plays the role of R_m in order to obtain the highest achievable value. Table 1 lists the parasitic values of an ideal OTRA and the CFOA-based one. To simplify the analysis, a reasonable assumption is made that R_{zn} are much greater than R_{xn} .

3. Single OTRA-Based Configuration

The first proposed general configuration is shown in Fig. 3a. It is operated via an input voltage signal n_i to produce a bistable output voltage n_o . The positive feedback loop is formed through the positive feedback network (PFN) from the output terminal to the non-inverting input of the OTRA. Thus, the OTRA saturates with its output voltage either at the positive saturation level L^+ or at the negative.

Saturation level $L^-(L^+=|L^-|)$. The PFN can be constructed by the combinations of different passive components.

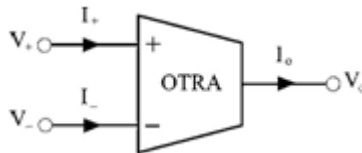


Figure 1: Circuit symbol of an OTRA

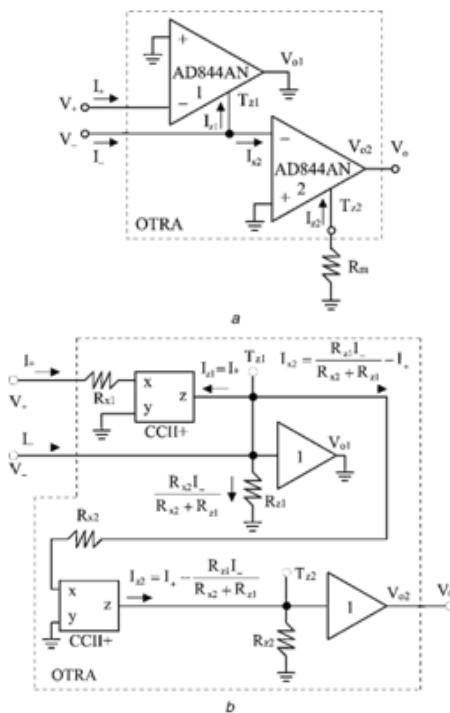


Figure 2: Implementation of an OTRA and equivalent circuit model. a. Implementation of an OTRA b. Non-ideal model of the applied OTRA

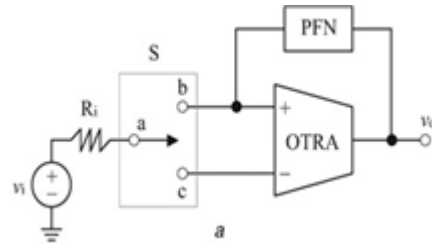


Figure 3: Characteristics of the OTRA-based configuration

a General single OTRA-based configuration b Transfer characteristic of the single OTRA-based configuration

From Fig. 3a, two feasible implementations are described as follows. When S is connected to the terminal c, the CW hysteresis characteristic can be achieved. If S is connected to the terminal b, the CCW hysteresis characteristic can be realized. A plot of the V_i - V_o transfer characteristic of the general single OTRA-based configuration is shown in Fig. 3b. It is assumed that the output level is at the positive saturation levels L^+ . For the CW hysteresis operation (see paths 1 and 2), as V_i increases from zero, V_o remains unchanged until V_i reaches the upper threshold voltage V_{TH} . Then, the OTRA will change its output level from L^+ to L^- . As long as V_i is greater than the lower threshold voltage V_{TL} , the output level remains at the negative saturation level. The CCW hysteresis with opposite operations is also displayed in Fig. 3b (see paths 1' and 2'). In the following sections, this general single OTRA-based configuration will be further studied with two typical examples.

4. Single-Resistor Topology

The single-resistor topology is shown in Fig. 4a. A resistor of R_1 is adopted to form the PFN. A voltage source and a resistor R_i form the input signal. In practice, the values of R_i and R_1 are selected to be much larger than the OTRA input impedances. The operations of this circuit are divided into two modes. For the CW-mode operation, the SPDT switch is connected to the terminal c. referring to Fig. 4a, the non-inverting input current I_p and the inverting input current I_2 can be expressed as

$$I_+ = V_o/R_1 + R_{x1} = V_o/R_1 \dots\dots\dots (2)$$

$$I_- = V_i/R_i + (R_{x2} || R_{z1}) = V_i/R_i \dots\dots\dots (3)$$

Assuming that no is at L^+ and V_i is smaller than V_{TH} initially, I^+ can be determined from (2) as

$$I_+ = L^+/R_1 \dots\dots\dots (4)$$

In Fig. 3b, n_i is now smaller than V_{TL} and n_o is at L^- . As n_i increases, I_p will increase too. The output level changes its state only when I_p is more positive than I_2 . Applying the same deductions as above, the upper threshold voltage V_{TH} can be derived as

$$V_{th} = (R_i/R_1)L^+ \dots\dots\dots (5)$$

5. Experimental Results

In the following tested prototype circuits, the saturation voltages are specified as $L^+=|L^-|=9.6V$. The input voltage

V_i is specified as a triangular wave with an amplitude of ± 10 V. For the design of the first proposed configuration shown in Fig. 3, the threshold voltages and the saturation levels are first specified. Substituting these parameters into (5) and the value of the ratio R_i/R_1 can be found. A feasible R_1 is chosen. Then, the value of R_i is obtained. For the single-resistor topology shown in Fig. 4a, the threshold voltages are defined as $V_{TH} = 4.8$ V and $V_{TL} = -4.8$ V. According to the design procedures, the ratio R_i/R_1 can be calculated as 0.5.

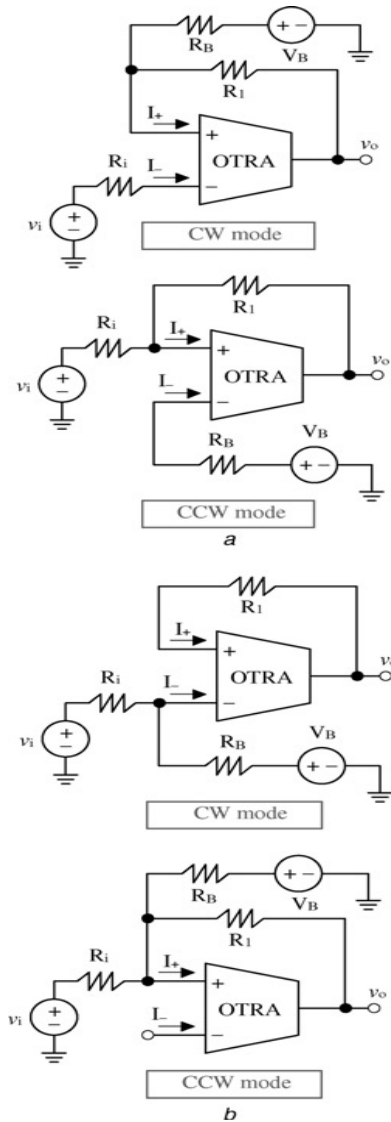


Figure 6: General single OTRA-based configurations
 a. With a positive switching voltage b. With a negative switching voltage

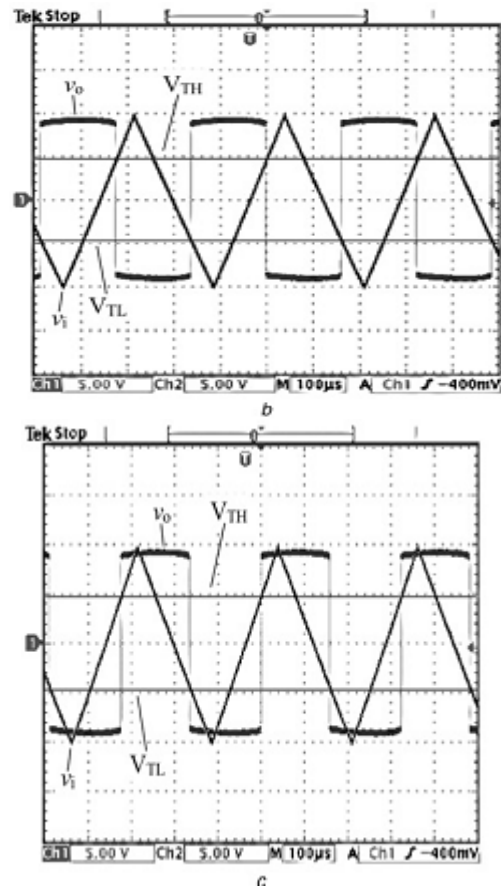
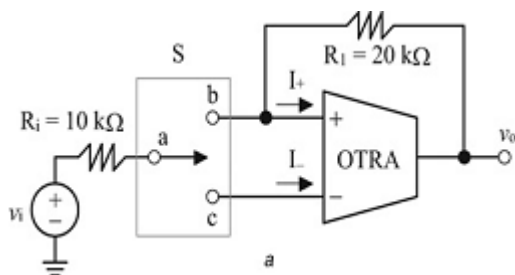


Figure 4: Experimental results for the single-resistor topology a. Circuit implementation b. CW mode c. CCW mode

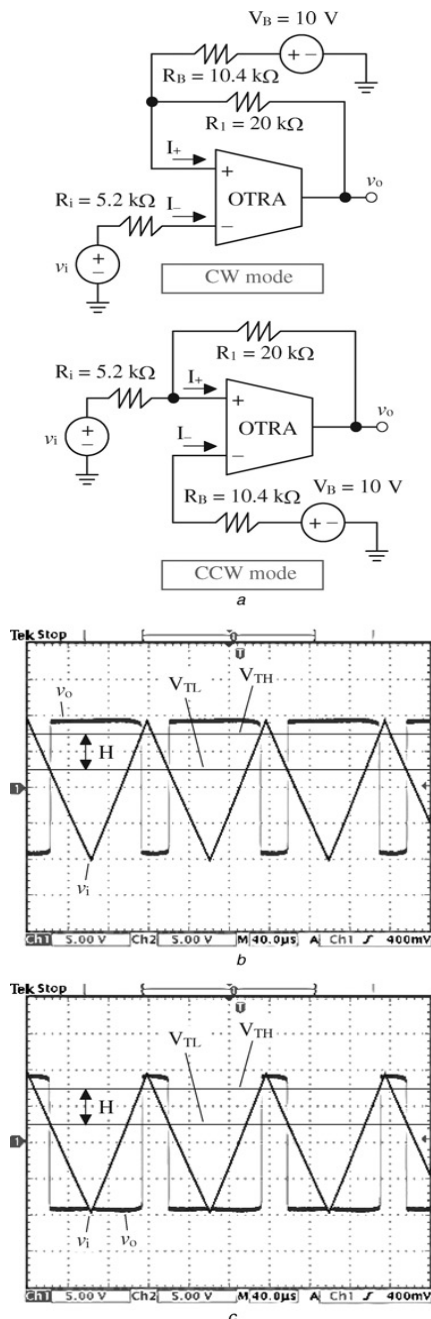


Figure 10: Experimental results for the topology with a positive switching voltage a Circuit implementations b CW mode c CCW mode

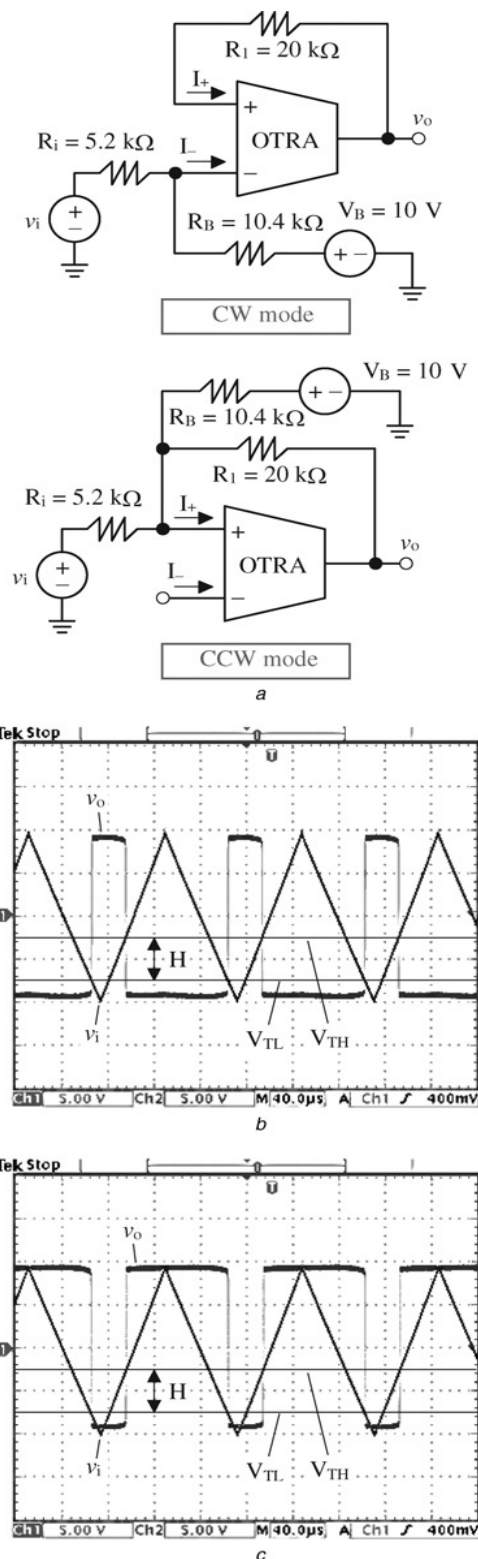


Figure 11: Experimental results for the topology with a negative switching voltage a. Circuit implementations b. CW mode c. CCW mode

6. Design Parameters and the Achieved Performances for the Proposed Circuits

Single-Resistor Topology CW/CCW Modes

1. Saturation voltages, $V : \pm 9.6V$
2. Other parameters : $R_i = 10K, 20K$
3. Threshold voltages $V_{TH}/V_{TL} = 4.8 V / -4.8 V$

4. Switching voltage $V_S, V = 0$
5. Hysteresis width $H, V = 9.6$

Diode-Resistor Topology CW/CCW Modes

Saturation voltages, $V = \pm 9.6V$

Other parameters: $R_i, R_1, R_2 = 10K, 20K$

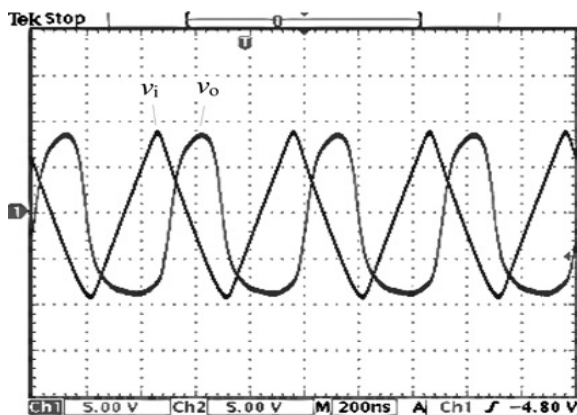
$V_{D1} V_{D2} = 0.7$

Threshold voltages $V_{TH}/V_{TL} = 4.45 V / -8.9 V$

$8.9 V / -4.45 V$

Switching voltage $V_S, V = -2.225 / 2.225$

Hysteresis width $H, V = 13.35$



Input and output waveforms with a frequency up to 2 MHz

OPA-Based [1]

1. Components: OPA X1 resistor X2
2. Electronically tunable: no
3. Hysteresis operation mode: single
4. Highest input frequency: tens of KHz

CCII-Based [2]

1. Components: CCIIx1, resistor 3
2. Electronically tunable: no
3. Hysteresis operation mode: single
4. Highest input frequency: hundreds of kHz

7. Comparisons of the Proposed OTRA-Based Circuits to other Bistable Multivibrators

OTRA-based

1. Components: OTRA x1 resistor x2
2. Electronically tunable: no
3. Hysteresis operation mode: Dual
4. Highest input frequency: Tens of MHz

8. Conclusion

In this paper, two novel bistable multivibrator configurations are presented. The proposed configurations are simple and versatile. Only one OTRA is required for each of the presented topology. Based on the two general configurations, a multiple-output general configuration is suggested to extend similar applications. The effectiveness of the proposed configurations has been verified through experimental results on prototype circuits. These circuits can be expected to find wide applications in communication and instrumentation systems.

References

- [1] Sedra A.S., Smith K.C.: 'Microelectronic circuits' (Oxford University Press, New York, 2004)
- [2] Dicaldo G., Palumbo G., Pennisi S.: 'A Schmitt trigger by means of a CCII β ', Int. J. Circuit Theory Appl., 1995, 23, pp. 161–165
- [3] Toumazou C., Lidegy F.J., Haigh D.: 'Analog IC design: the current-mode approach' (Peter Peregrinus, Exeter, UK, 1990)
- [4] Smith K.C., Sedra A.S.: 'The current conveyor: a new circuit building block', Proc. IEEE., 1968, 56, pp. 1368–1369
- [5] Fakhfakh M., Loulou M., Tlelo-Cuautle E.: 'Synthesis of CCII and design of simulated CCII based floating inductances', IEEE ICECS, 2007, pp. 379–382
- [6] Maundy B.J., Sarkar A.R., Gift S.J.: 'A new design topology for low-voltage CMOS current feedback amplifiers', IEEE Trans. Circuits Syst. II, 2006, 53, (1), pp. 34–38
- [7] Alzahrer H., Ismail M.: 'A CMOS fully balanced differential difference amplifier and its applications', IEEE Trans. Circuits Syst. II, 2001, 48, (6), pp. 614–620
- [8] Elwan H.O., Soliman A.M.: 'Novel CMOS differential voltage current conveyor and its applications', IEE Proc., Circuits Devices Syst., 1997, 144, (6), pp. 195–200
- [9] El-Adawy A.A., Soliman A.M., Elwan H.O.: 'A novel fully differential current conveyor and applications for analog VLSI', IEEE Trans. Circuits Syst. II, 2000, 47, (4), pp. 306–313
- [10] Ray B.N., Nandi P.K., Chaudhuri P.P.: 'Synthesis of programmable multi-input current-mode linear analog circuits', IEEE Trans. Circuits Syst. I, 2004, 51, (8), pp. 1440–1456
- [11] Chang C.M.: 'Analytical synthesis of the digitally programmable voltage-mode OTA-C universal biquad', IEEE Trans. Circuits Syst. II, 2006, 53, (8), pp. 607–611
- [12] Cakir C., Cam U., Cicekoglu O.: 'Novel all pass filter configuration employing single OTRA', IEEE Trans. Circuits Syst. II, 2005, 52, (3), pp. 122–125
- [13] Salama K.N., Soliman A.M.: 'Novel oscillators using the operational transresistance amplifier', Microelectron. J., 2000, 31, (1), pp. 39–47

Author Profile



J. Chandra Shekhar is working as Assistant Professor in the Department of E.C.E in MLR Institute of Technology. Interested areas in Electromagnetic waves and Antenna wave propagation.



G. Shravan Kumar is working as Assistant Professor in the Department of E.C.E in MLR Institute of Technology. M.Tech in VLSI & ES. Interested areas for Research are Signal Processing and VLSI.